Ultrahigh Bandwidth Spin Noise Spectroscopy: Detection of Large g-Factor Fluctuations in Highly-n-Doped GaAs

Fabian Berski,* Hendrik Kuhn, Jan G. Lonnemann, Jens Hübner,† and Michael Oestreich‡

Institut für Festkörperphysik, Leibniz Universität Hannover, Appelstraße 2, D-30167 Hannover, Germany

(Received 29 June 2012; revised manuscript received 7 August 2013; published 29 October 2013)

We advance all optical spin noise spectroscopy (SNS) in semiconductors to detection bandwidths of several hundred gigahertz by employing a sophisticated scheme of pulse trains from ultrafast laser oscillators as an optical probe. The ultrafast SNS technique avoids the need for optical pumping and enables nearly perturbation free measurements of extremely short spin dephasing times. We apply the technique to highly-n-doped bulk GaAs where magnetic field dependent measurements show unexpected large g-factor fluctuations. Calculations suggest that such large g-factor fluctuations do not necessarily result from extrinsic sample variations but are intrinsically present in every doped semiconductor due to the stochastic nature of the dopant distribution.

DOI: 10.1103/PhysRevLett.111.186602 PACS numbers: 72.25.Rb, 72.70.+m, 78.47.db, 85.75.−d

Spin noise spectroscopy (SNS) has proven itself as a well-developed experimental technique in semiconductor spin quantum optronics [1–3]. The low perturbing nature of SNS makes the technique an ideal tool to study the unaltered long coherence times of electron spins in semiconductors [4] and semiconductor nanostructures [2,5]. However, short spin coherence times require a high detection bandwidth, and thus the temporal capabilities of cw SNS are limited by the speed of the electro-optic conversion [6]. This limit is currently with the most modern electronics at about 1 GHz [7]. A first successful step to overcome this limitation has been made by employing a single ultrafast laser oscillator as a stroboscopic optical sampling tool, which directly enabled spin noise measurements of frequencies up to several GHz, but with a fixed bandwidth of roughly 0.1 GHz [8]. In this Letter, we report the first experimental demonstration of spin noise spectroscopy with a full bandwidth that is increased by several orders of magnitude to nearly 100 GHz, which corresponds to spin dephasing times in the picosecond regime. Thereby, the presented SNS method is ideally suited for systems which intrinsically show a fast decay of spin coherence and are yet susceptible to optical excitation, like hole spin systems with a high degree of spin-orbit interaction [9], carrier systems at very low temperatures (<100 mK), or Bose-Einstein condensation of magnons [10].

In the following, we employ the technique of ultrafast SNS to highly-n-doped bulk GaAs and find in the metallic regime large g-factor fluctuations. Calculations reveal that these large g-factor fluctuations are an intrinsic bulk property of doped semiconductors. The effect results from the stochastic distribution of donor atoms and the imperfect local averaging of electrons due to their finite momentum and spin dephasing times [11]. Ultrafast SNS asserts itself as the perfect tool to measure such an effect since it combines the necessary high temporal resolution, negligible disturbance of the system, and efficient averaging over very large sample volumes compared to other optical methods due to the below-band-gap detection.

The extended measurement principle of ultrafast SNS is based upon the repeated measurement of the correlated Faraday rotation signal $\theta(t_i)\theta(t_i + \Delta t)$ of two ultrashort laser probe pulses with a temporal delay of Δt [12]. The point in time t_i is arbitrary for every pulse pair due to the stochastic nature of the spin dynamics if the repetition period between two pulse pairs is much larger than the spin dephasing time. The average Faraday rotation signal $\langle\theta\rangle(\Delta t)$ vanishes if the nonmagnetic sample is in thermal equilibrium. However, the variance $\sigma^2_\theta(\Delta t)$ is not zero but is maximal for fully correlated Faraday rotation of the two laser pulses ($\Delta t = 0$), decreases with increasing Δt to a finite value due to spin dephasing, oscillates with Δt in the presence of a transverse magnetic field B due to Larmor precession of the electron spins, and approaches zero for anticorrelation.

In this work, the sampling pulses are delivered by two synchronized, ultrafast, picosecond laser oscillators with a common repetition rate of 80 MHz [13]. The relative phase between the two emitted pulse trains is adjustable, so that pairs consisting of two laser pulses are formed with a temporal delay Δt which can be conveniently tuned between a picosecond and a few nanoseconds. The correlated Faraday rotation signal of both pulses within a pulse pair is measured by a balanced detector which is so slow that it integrates over each pulse pair but is fast enough to distinguish two succeeding pulse pairs. In other words, the Faraday rotation signals of the two pulses of a pulse pair are added up for $\Delta t \lesssim 12.5$ ns but the fluctuation from pulse pair to pulse pair is fully resolved. A rectification of the Faraday signal is implemented by taking the square of $\theta(t_i) + \theta(t_i + \Delta t)$ during the data acquisition. The experimental setup is depicted in Fig. 1. The two degenerate, linearly polarized laser pulses are combined in a polarization maintaining, single mode fiber to ensure a common

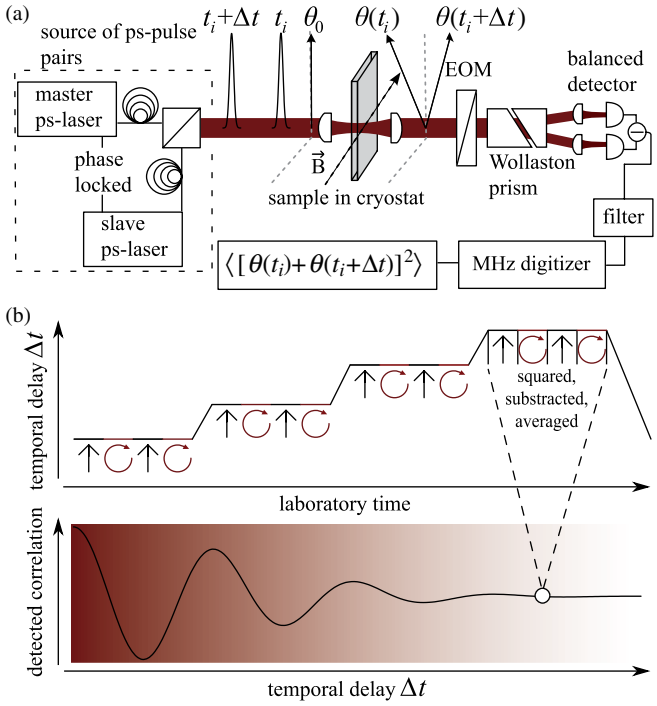

FIG. 1 (color online). (a) Experimental setup: The outputs of two synchronized ps laser oscillators are combined via a single mode optical fiber and transmitted through the sample (gray region) which is mounted in a magneto-optical cryostat (not shown). The rotation of the linear input polarization θ_0 is analyzed behind the sample with a polarization bridge and a balanced photoreceiver. Here, $\theta(t_i)$ and $\theta(t_i + \Delta t)$ denote the stochastic rotation of the two individual laser pulses after the sample. The amplified electrical signal is digitized and seamlessly analyzed on a standard computer. (b) Schematic measurement sequence. Details are given in the text.

beam profile in addition to identical pulse length, power, and wavelength. The probe laser light has an average power of 17 mW and is focused to a spot diameter of about 50 μm onto the sample surface. After traversing the sample, the spin induced fluctuations of the linear polarization are analyzed by a polarization bridge given by a $\frac{1}{2}\lambda$ wave plate for power balancing, a Wollaston prism, and a low noise, differential, optical photoreceiver with a 3 dB bandwidth of 160 MHz. The electrical output of the photoreceiver is passed through a dc and a low pass filter with a cutoff frequency of 70 MHz before being amplified in order to suppress any residual voltage peaks arising from the limited common noise rejection of the differential photoreceiver. Finally, the filtered signal is digitized by a 160 Msample/s digitizer card and sent to a personal computer for further processing.

The measured signal is not only composed of pure spin noise but also of residual background contributions, which are mainly caused by optical shot noise. The spin noise is extracted by using an electro-optical modulator (EOM) before the polarization bridge, which acts either as a $\frac{1}{4}\lambda$ or as a 0λ retarder with a square wave modulation of 4 kHz. For 0λ retardance, the EOM transmits the incoming polarization unchanged (spin noise is detected), but for $\frac{1}{4}\lambda$ retardance, every off-axis polarization component is transformed into elliptically polarized light and divided into two equal parts at the polarization bridge (no spin noise is detected; background only). This fast background acquisition strongly suppresses any parasitic fluctuations and yields an extremely reliable data series. The measurement protocol is depicted in Fig. 1(b): A single measurement window is 100 ms long. The start and end points are set in the presented measurement to 80 and 835 ps, respectively [14]. The time delay is increased in 96 steps with a step length of 1 ms. The exact time delay for each step has been verified with a calibrated streak camera system. During each step, the EOM switches four times between $\frac{1}{4}\lambda$ and 0λ retardance.

The first sample is Czochralski grown, bulk GaAs:Te with a nominal n-doping concentration of $n_d = 8.2 \times 10^{17}$ cm^{-3} and a thickness of $d \approx 300$ μm. The second sample under study is 4 times lower doped GaAs:Si with $n_d = 2.1 \times 10^{17}$ cm^{-3}, has the same thickness, and both surfaces are coated with antireflection material. The high doping concentrations yield a metallicline conduction band with Fermi levels of $E_F = 47.7$ meV and $E_F = 19.2$ meV above the conduction band minimum, respectively. The dominant origin of spin dephasing is for both samples the Dyakonov-Perel mechanism [15] since the energy dependent spin splitting of the conduction band is large in GaAs at such high Fermi energies. In the following, we focus first on the higher doped sample with an expected spin dephasing time on the order of a few hundred picoseconds [11].

The top panel of Fig. 2 shows the derivative of the measured (dots) spin correlation $(d/d\Delta t)\sigma_\theta^2$ as a function of the temporal pulse delay Δt for sample 1. The derivative has been taken to suppress a slow varying background slope with Δt which originates from the coupling of the two independent laser sources by a lock-to-clock system [16]. Assuming a free induction decay of the free precessing electrons $\cos(\omega_L t)e^{-t/\tau_s}$, the derivative of the autocorrelation is given by

$$\frac{d}{d\Delta t}\sigma_\theta^2 \propto \{\omega_L \tau_s \sin(\omega_L \Delta t) + 2\cos(\omega_L \Delta t)\}e^{-\Delta t/\tau_s}, \quad (1)$$

where $\omega_L = \hbar^{-1} g^* \mu_B B$ is the Larmor precession frequency with g^* as the effective electron g-factor and τ_s is the spin dephasing, i.e., spin correlation, time. The red line in the top panel of Fig. 2 is a fit with Eq. (1) which matches with very high accuracy. Please note that the extrapolation to time delay zero indicates a positive extremum, which perfectly corresponds to the expected maximum correlation.

The bottom panel of Fig. 2 shows the extracted dependence of $\tau_s(B)$ on the applied transverse magnetic field strength B. The spin dephasing time at vanishing field

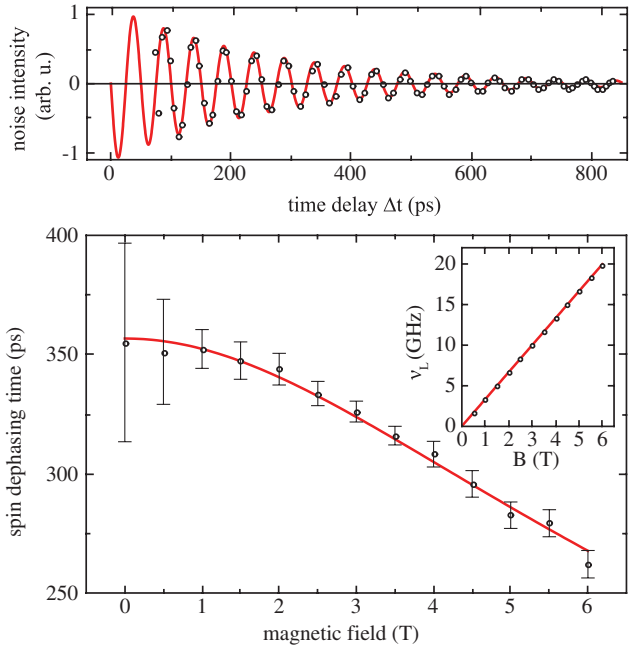

FIG. 2 (color). Top: Spin correlation derivative (dots) of free electron spins precessing in a transverse magnetic field of 6 T, probe laser energy of 1.514 eV, and $T = 20$ K. The red line is a fit to the data according to Eq. (1). The average full bandwidth is set to 60 GHz by the chosen time step. Bottom: Dependence of spin dephasing time τ_s on the transverse magnetic field strength. The red line is a fit by Eq. (2) with parameters listed in the text. The inset shows the measured change of the Larmor frequency ν_L with magnetic field (black dots) and a linear fit by $\nu_L = g^* \mu_B B/h$ (red line) which yields the effective electron Landé g-factor.

$\tau_s(0) \approx 360$ ps corresponds well to the expected spin dephasing time limited by the Dyakonov-Perel spin dephasing mechanism [11]. Surprisingly, the spin dephasing time decreases with increasing magnetic field due to a significant inhomogeneous spread of the electron Landé g-factor. The red line is a fit given by the inverse width w_v of an approximated Voigt profile according to

$$\tau_s(B) = (\pi w_v)^{-1} \approx \frac{1}{\pi}\left[c_0\gamma_h + \sqrt{c_1\gamma_h^2 + (\gamma_i/\pi)^2}\right]^{-1}, \tag{2}$$

where γ_h and γ_i are the homogenous and inhomogeneous spin dephasing rates, respectively, and c_0 and c_1 are constants [18]. The homogeneous spin dephasing rate of the monoexponential decay is given by $\gamma_h = 1/\tau_s(0)$ [6]. The inhomogeneous spin dephasing rate γ_i is directly linked to the standard deviation of the g-factor spread σ_g by $\gamma_i = \sigma_g \mu_B B/\hbar$. From the fit to Eq. (2) with $\tau_s(0)$ and σ_g as free parameters, we obtain a g-factor variation $\sigma_g = 0.0034$ which is surprisingly large, taking into account that all valence electrons are well in the metallic state. We will explain the possible origin of this phenomenon in the next paragraph. The inset of the bottom of Fig. 2 depicts the dependence of the Larmor precession frequency on B. The relative measurement error of the Larmor frequency is smaller than 10^{-4} for $B \geq 2$ T while the absolute error is about $\pm 1\%$ due to errors in the absolute calibration of B and Δt. The nearly perfect fit to a straight line yields the magnitude of the average free electron Landé g-factor which is $g^* = -0.236$. The negative sign is assigned from the relation $g^* = -0.48 + \beta E_F$. We determine the factor β which reflects the energy dependence of the Landé g-factor to $\beta \approx 5.1$ eV^{-1} for this doping concentration and attribute the deviation from the commonly known factor of 6.3 eV^{-1} for slightly doped samples [20,21] to band-gap renormalization arising from the high doping concentration. The deviation of g^* being a constant is less than 10^{-3} T^{-1} which is at least a factor of 5 lower than for low doped GaAs at low temperatures.

Next, we discuss the origin of σ_g. Most interestingly, the measured g-factor variation in metallic bulk semiconductors can be attributed to an intrinsic contribution which arises from the pure thermodynamic distribution of dopant atoms in the material during growth: The Fermi level is inherently constant over the entire sample, but the stochastic fluctuations of the dopant concentration give rise to local space charge densities [22] which in turn shift the band structure with respect to the Fermi level. To first approximation, an electron propagates in this local inhomogeneity undisturbed over an average distance $\bar{r} = v_f \tau_p/2$, where τ_p is the electron momentum scattering time and $v_f = \sqrt{2E_F/m^*}$ is the Fermi velocity. At low temperatures, ionized impurity scattering is the main scattering mechanism for highly doped bulk semiconductors. The momentum scattering time can easily be extracted from the spin dephasing time measured at zero magnetic field by the relation [23,24]

$$\tau_s^{-1} = \frac{32}{105}\gamma_3^{-1}\alpha^2\frac{E_F^3}{\hbar^2 E_g}\tau_p, \tag{3}$$

with $\gamma_3 = 6$ for ionized impurity scattering and $\alpha = 0.07$ [25]; E_g is the energy gap. We determine from the measured $\tau_s(0) \approx 360$ ps an average momentum scattering time of 70 fs, which is very reasonable for this kind of sample and scattering mechanism [24]. An electron samples an average volume $\bar{V} = (4\pi/3\bar{r}^3)(\tau_s/\tau_p)$ during τ_s on its diffusive scattering path, which amounts roughly to $\bar{V} \approx 0.1\ \mu$m^3 for the given conditions. For each electron, the number of donor atoms within this volume fluctuates with $\sqrt{\bar{V}n_d}$. The resulting change in the local doping density is directly linked to the g-factor variation via the energy dependence of the g-factor, as shown above. We calculate for the given doping density in sample 1 an intrinsic g-factor variation due to the

local doping density fluctuations of $\sigma_g = 5 \times 10^{-4}$. The experimental value is only a factor of 6 higher than that obtained by this straightforward approximation.

Certainly, other inhomogeneities may contribute to the measured g-factor fluctuation, and the theoretical description is only an order of magnitude estimation [26]. Nevertheless, a statistical distribution of donor atoms is inevitably present in doped semiconductors, and the estimated effect on σ_g is large. The effect is, in particular, orders of magnitude larger than the familiar variable g-factor mechanism due to electrons in different quantum states at the Fermi edge [27].

Next, we want to corroborate our model by a density dependent measurement. The model links σ_g to the doping density and the measured zero field spin dephasing time by [28]

$$\sigma_g \propto \frac{\partial E_F}{\partial n_d}\bigg|_{n_d} \delta n \propto n_d^{2/3}\sqrt{\tau_s(0)}. \quad (4)$$

We measure for the lower doped sample 2 a spin lifetime $\tau_s(0) = 980$ ps and a g-factor fluctuation of $\sigma_g = 0.0028$. The significantly longer $\tau_s(0)$ is in excellent agreement with the Dyakonov-Perel spin relaxation mechanism [11]. More importantly, the measured σ_g is significantly reduced in the lower doped sample by 18%, as qualitatively predicted by our model. The quantitative agreement between calculated and measured reduction is reasonably good, i.e., the calculated reduction corresponds to a ratio of ≈ 0.63, and the measured ratio is ≈ 0.82.

In conclusion, we successfully demonstrated ultrafast spin noise spectroscopy and increased the state of the art bandwidth by more than 2 orders of magnitude. The bandwidth is in principle only limited by the pulse width of the laser and should reach the THz regime for femtosecond laser pulses [29]. Already, the demonstrated bandwidth of 60 GHz enables SNS measurements on systems with picosecond spin dynamics. This applies for, e.g., magnons in yttrium iron garnet, hole spin systems at very low temperatures, as well as for many-electron systems at room temperature. Here, we applied ultrafast SNS to highly-n-doped bulk GaAs well above the metal-to-insulator transition, which is the archetype material for spintronics, and observed, despite being in the metallic regime, a large g-factor fluctuation. Calculations and measurements on two different samples show that such large g-factor fluctuations are intrinsic to doped semiconductors and result from the inevitable stochastic variation of the doping concentration.

We acknowledge the financial support by the BMBF joint research project QuaHL-Rep, the Deutsche Forschungsgemeinschaft in the framework of the priority program "SPP 1285—Semiconductor Spintronics," and the excellence cluster "QUEST—Center for Quantum Engineering and Space-Time Research." The authors F. B. and H. K. contributed equally to this work.

*Berski@nano.uni-hannover.de
†jhuebner@nano.uni-hannover.de
‡oest@nano.uni-hannover.de

[1] G. M. Müller, M. Oestreich, M. Römer, and J. Hübner, Physica (Amsterdam) **43E**, 569 (2010).
[2] R. Dahbashi, J. Hübner, F. Berski, J. Wiegand, X. Marie, K. Pierz, H. W. Schumacher, and M. Oestreich, Appl. Phys. Lett. **100**, 031906 (2012).
[3] S. A. Crooker, L. Cheng, and D. L. Smith, Phys. Rev. B **79**, 035208 (2009).
[4] M. Römer, H. Bernien, G. Müller, D. Schuh, J. Hübner, and M. Oestreich, Phys. Rev. B **81**, 075216 (2010).
[5] G. M. Müller, M. Römer, D. Schuh, W. Wegscheider, J. Hübner, and M. Oestreich, Phys. Rev. Lett. **101**, 206601 (2008).
[6] M. Römer, J. Hübner, and M. Oestreich, Rev. Sci. Instrum. **78**, 103903 (2007).
[7] S. A. Crooker, J. Brandt, C. Sandfort, A. Greilich, D. R. Yakovlev, D. Reuter, A. D. Wieck, and M. Bayer, Phys. Rev. Lett. **104**, 036601 (2010).
[8] G. M. Müller, M. Römer, J. Hübner, and M. Oestreich, Phys. Rev. B **81**, 121202(R) (2010).
[9] M. Wu, J. Jiang, and M. Weng, Phys. Rep. **493**, 61 (2010).
[10] S. O. Demokritov, V. E. Demidov, O. Dzyapko, G. A. Melkov, A. A. Serga, B. Hillebrands, and A. N. Slavin, Nature (London) **443**, 430 (2006).
[11] R. I. Dzhioev, K. V. Kavokin, V. L. Korenev, M. V. Lazarev, B. Y. Meltser, M. N. Stepanova, B. P. Zakharchenya, D. Gammon, and D. S. Katzer, Phys. Rev. B **66**, 245204 (2002).
[12] S. Starosielec and D. Hägele, Appl. Phys. Lett. **93**, 051116 (2008).
[13] Without loss of applicability, one ultrafast laser together with a mechanical delay stage can be used instead of two ultrafast lasers.
[14] The minimum time delay of 80 ps results from technical limitations of the currently used balanced receiver. The rather slow photodiodes of the receiver show a nonlinear electrical response for short time delays, whereby a more elaborate data processing is needed. A detector with much faster photodiodes will significantly reduce this issue.
[15] M. I. Dyakonov and V. I. Perel, Sov. Phys. Solid State **13**, 3023 (1972).
[16] A free running ultrafast rapid temporal delay scanning scheme circumvents this background but raises other constraints, which are discussed in detail in Ref. [17].
[17] J. Hübner, J. G. Lonnemann, P. Zell, H. Kuhn, F. Berski, and M. Oestreich, Opt. Express **21**, 5872 (2013).
[18] $c_0 = 0.5346$ and $c_1 = 0.2166$ [19].
[19] J. Olivero and R. Longbothum, J. Quant. Spectrosc. Radiat. Transfer **17**, 233 (1977).
[20] M. A. Hopkins, R. J. Nicholas, P. Pfeffer, W. Zawadzki, D. Gauthier, J. C. Portal, and M. A. DiForte-Poisson, Semicond. Sci. Technol. **2**, 568 (1987).
[21] J. Hübner, S. Döhrmann, D. Hägele, and M. Oestreich, Phys. Rev. B **79**, 193307 (2009).
[22] M. M. Glazov, M. A. Semina, and E. Y. Sherman, Phys. Rev. B **81**, 115332 (2010).

[23] G. E. Pikus and A. N. Titkov, in *Optical Orientation*, edited by F. Meier and B. P. Zakharchenya (North-Holland, Amsterdam, 1984), p. 109.
[24] I. Žutić, J. Fabian, and S. D. Sarma, Rev. Mod. Phys. **76**, 323 (2004).
[25] V. A. Marushchak, M. N. Stepanova, and A. N. Titkov, Sov. Phys. Solid State **25**, 2035 (1983).
[26] We also measured a lateral variance of the average g factor of $\approx 9.6 \times 10^{-4}$ by spatially changing the transmission spot on sample 1. This lateral variance is more than a factor of 3 smaller than the measured σ_g and gives an upper limit for the measurement uncertainty.
[27] F. X. Bronold, I. Martin, A. Saxena, and D. L. Smith, Phys. Rev. B **66**, 233206 (2002).
[28] Equipollently, $\tau_s(0)$ can be expressed by τ_p and n_d.
[29] At very short laser pulses, coherent electronic processes in the sample and in the balanced receiver might influence the spin noise signal.